Thermal studies and magnetic properties of mechanical alloyed Fe$_2$B

Thermal studies and magnetic properties of mechanical alloyed Fe$_2$B

E C Passamani[1]**, J R B Tagarro, C Larica and A A R Fernandes**

Universidade Federal do Espírito Santo, Depto. de Física, Vitória, ES 29060900, Brazil

E-mail: edson@cce.ufes.br

Abstract
In the present paper, a high energy milling process has been used to alloy Fe
and B in the proportion 2:1. X-ray diffraction and Mössbauer spectroscopy
were used to follow the solid state reaction among the alloy components and
phase formation during thermal treatments of the final milled alloy, at distinct
temperatures and environments. X-ray, DSC and Mössbauer data of the 310 h
milled alloy show the presence of three phases: small fractions of α-Fe (n-Fe)
and Fe$_2$B (n-Fe$_2$B) nanocrystalline phases and a large amount of amorphous
Fe$_2$B (a-Fe$_2$B) phase (73%). Heat treatment of the milled alloy was done in
a high vacuum furnace, followed by *in situ* Mössbauer measurements, or by
annealing the sample sealed in a quartz tube. It is shown that segregation and
crystallization effects thermally induced in the samples have been enhanced by
the presence of oxygen in the residual atmosphere, being less effective in the
case where the sample was continuously pumped during the annealing. These
effects may have occurred due to boron oxidation. Also, the presence of a *tet*-
Fe$_3$B phase in the annealed samples has been observed. The high temperature
Mössbauer spectra for the sample annealed at 823 K indicate that the n-Fe$_2$B,
n-Fe$_3$B and n-Fe phases exhibit superparamagnetic behaviour, with estimated
blocking temperatures of 723 and 823 K, respectively. The amorphous a-Fe$_2$B
phase has a T_C value estimated at about 823 K that fits into the system reported
for amorphous Fe/B ribbons.

1. Introduction

Amorphous Fe/B and related alloys exhibit attractive soft magnetic properties and are an
important system to be investigated. Fe/B amorphous (a-Fe/B) alloys have been produced by
several distinct methods, such as liquid quenched (Chien *et al* 1979, Shánchez *et al* 1992)
and high energy milling (HEM) (Jing *et al* 1991, Yang *et al* 1999). Recently, HEM has been

---

[1] Author to whom any correspondence should be addressed.

applied to produce a-Fe/B alloys starting from a mixture of chemical elemental powders (Jing *et al* 1991, Yang *et al* 1999) and from a Fe_2B ordered compound (Balogh *et al* 1997). Reports on the formation of an amorphous Fe/B alloy produced by HEM are not consistent: (a) Yang *et al* (1999) have shown that the single amorphous phase can only be obtained by milling the Fe_xB_{1-x} alloy, with nominal composition $x = 60$, under an argon atmosphere, otherwise the amounts of the Fe-like and Fe_2B crystalline phases are higher than the amorphous phase; (b) Jing *et al* (1991) have shown an almost single nanocrystalline phase for the $Fe_{66}B_{34}$ alloy produced by HEM, while a mixture of crystalline and amorphous phases are obtained for boron compositions higher than 34 at%, and finally (c) Balogh *et al* (1997) have shown that, applying the HEM technique to the Fe_2B ordered compound, the amorphous state is not yielded. In the latter case, the presence of a α-Fe phase observed in the milled alloy was attributed to iron contamination from the milling tools.

Discrepancies reported in the properties of milled materials, as for those mentioned above, are frequently observed in the literature (e.g. Larica *et al* 1995, Waba and Shiba 1993). From our point of view, the amount of phases present in milled alloys depends basically on the milling conditions, i.e. the type of milling machine, the local residual atmosphere, the tool to powder ratio, etc. In the present case, it is intended to show that the preparation of the amorphous Fe/B alloy with a specific milling tool led to a large amount of amorphous phase compared to those reported by Jing *et al* (1991) and Yang *et al* (1999), where nanocrystalline phases present in their milled alloys are the dominant ones. Also some elucidative considerations will be pointed out associated with: (a) the Fe segregation and Fe_3B crystallization effects observed in different annealing processes and (b) high temperature magnetic properties for the amorphous and nanocrystalline Fe/B phases.

2. Experimental details

The $Fe_{67}B_{33}$ alloy was obtained by milling 14 g of a mixture of high purity (99.999%) elemental powders of crystalline α-Fe and amorphous B for a period of 310 h (sample A). The initial elemental powder mixture was sealed, under high purity Ar atmosphere (6 N), in a hard steel vial and clamped in a commercial vibrating frame machine. The milling tool used here was a massive cylinder of the same material as the vial, occupying 63% of total internal space. More details of the milling tools and experimental procedures have already been reported by Larica *et al* (1995). Powder samples were collected at pre-defined milling times in order to investigate the alloying process. The powder manipulations were always done inside a glove box under high purity argon atmosphere.

Part of sample A was sealed in a high vacuum Mössbauer furnace and heat treated in the temperature range from 350–823 K, at a vacuum better than 7×10^{-6} Torr by continuously pumping with a turbo molecular pump. The sample was submitted for 2 h heat treatments, at several temperature values 50 K apart. After each temperature step the sample was cooled down to 300 K for Mössbauer measurement (sample B). Also, three other parts of sample A were sealed in a Ta foil and then encapsulated in separate quartz tubes, at an initial vacuum better than 7×10^{-6} Torr, for heat treatment at 423, 623 and 923 K, in a tubular resistive furnace, for a period of approximately 2 h (sample C). In both experiments, the heating and cooling rates were nearly the same and kept close to 5 K min^{-1}.

EDS analysis has been performed on sample A and no Cr contamination has been detected and the Fe/B composition was closely maintained.

X-ray diffraction (XRD) patterns were obtained for all samples with Cu Kα radiation at room temperature (RT).
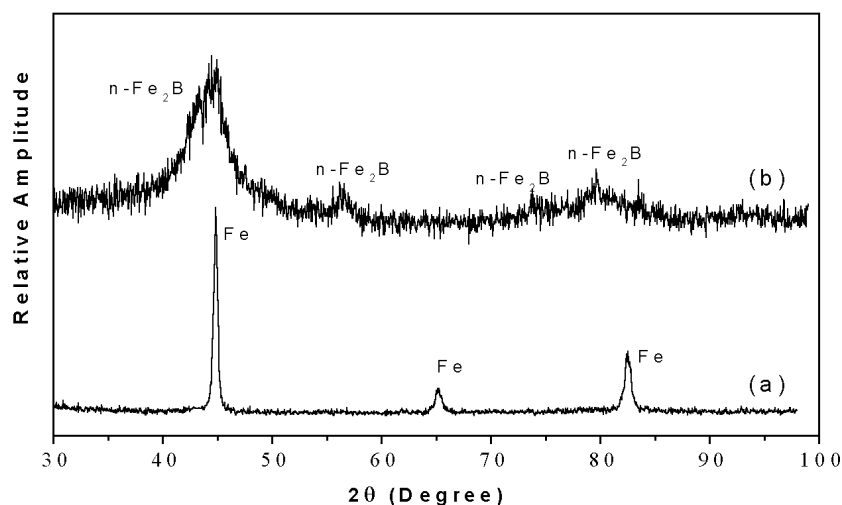
Figure 1. XRD patterns of the $Fe_{67}B_{33}$ alloy: (*a*) non-milled alloy, (*b*) milled for 310 h (sample A).

Differential scanning calorimetry (DSC) analysis was performed in a Shimadzu DSC-50 between 300–900 K. About 10 mg of the milled material was enclosed in an aluminium pan covered with an aluminium lid (an empty pan with lid was used as reference). The signal was recorded in the heating ramps, with a heating-rate of 20 K min^{-1}, under an argon flux of 30 ml min^{-1}.

All ^{57}Fe Mössbauer spectra of the as-milled and annealed Fe₂B powders were measured at 300 K with a 25 mCi ^{57}Co:Rh radioactive source in conventional transmission geometry. Also, *in situ* high temperature Mössbauer spectra of sample B have been obtained in a high vacuum furnace after this sample had been annealed at 823 K for 2 h. In this experiment the source and absorber were kept at different temperatures. The isomer shift (IS) values are given relative to α-Fe at RT.

3. Results and discussions

Figure 1 shows the XRD patterns of the non-milled $Fe_{67}B_{33}$ mixture and sample A ($Fe_{67}B_{33}$ alloy milled for 310 h). The XRD pattern of the mixture (figure 1(*a*)) displays only the Bragg peaks of the bcc-Fe phase, an expected result since the boron phase is in an amorphous state. The XRD pattern of sample A (figure 1(*b*)) shows broad reflection lines at angular positions of the α-Fe and Fe₂B phases. The appearance of the Fe₂B Bragg reflection lines, in the XRD patterns, was observed for milling times longer than 10 h. Thus, the x-ray result of sample A may only indicate the presence of two nanocrystalline phases in sample A: n-Fe and n-Fe₂B.

However, DSC measurements, shown in figure 2, display a strong irreversible exothermic peak at about 835 K, which is generally associated with an amorphous–crystalline transition (Chong-Oh *et al* 1981). The two weak exothermic peaks observed in the DSC curve, at about 650 and 735 K, are often found for a-Fe/B materials and they had been associated with a structural relaxation effect or due to an early surface crystallization process (particle surfaces process) (Jing *et al* 1991). The presence and the fraction of an amorphous Fe/B (a-Fe/B) phase will be better understood from the results of Mössbauer spectoscopy discussed below.
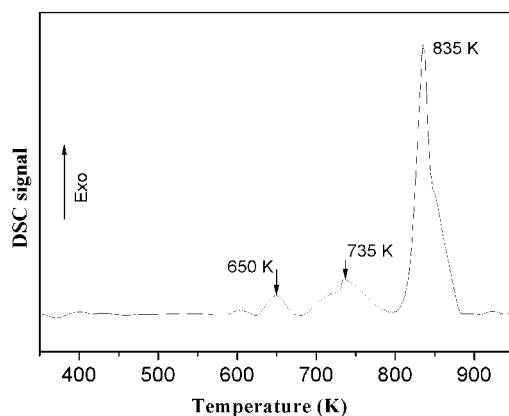
Figure 2. DSC curve of the $Fe_{67}B_{33}$ alloy milled for 310 h (sample A).

Figure 3 displays the Mössbauer spectra taken at 300 K of samples A and B, the latter annealed at different temperatures. The sample A spectrum was fitted with two sextets (S1 and S2), having their hyperfine parameters close to those of α-Fe (IS ≈ -0.01 mm s^{-1} and $B_{hf} \approx 33.0$ T) and Fe_2B (IS ≈ 0.17 mm s^{-1}, $B_{hf} \approx 23.5$ T and QS ≈ 0.04 mm s^{-1}) phases, respectively, in agreement with the XRD results, plus a magnetic hyperfine field distribution subspectrum, having the IS and the most probable B_{hf} values close to those hyperfine values of the S2 subspectrum (Fe_2B). Therefore, the magnetic hyperfine field distribution component may be associated with an amorphous $Fe_{67}B_{33}$ alloy (a-Fe_2B), consistent with the amorphous–crystalline transition, observed in the DSC experiment, associated with the exothermic peak at 835 K (figure 2). Usually, the Mössbauer spectrum of the ordered Fe_2B phase is fitted with two magnetic sextets, having combined magnetic and electric interactions, with similar IS values, but slightly different B_{hf} and QS values (Murphy and Hershwowitz 1973). However, ordered phases submitted to an HEM process may have a large number of defects, resulting in a broad sextet, which makes the two Fe sites indistinguishable. Xia *et al* (1996) have shown this effect for the Fe_2Sc compound, after short milling times, where the long-range crystalline order has been strongly reduced by the mechanical cold work. For the same reason, in the present case the nanocrystalline Fe_2B phase (n-Fe_2B) has been fitted with one slightly broad sextet having its hyperfine parameters close to the average values of the sextets observed for the ordered Fe_2B phase (Murphy and Hershwowitz 1973).

The 300 K Mössbauer spectra of sample B have been fitted with the same three magnetic subspectra used to fit the sample A case, but varying their relative volume fractions for different annealing temperatures.

Figure 4 summarizes the thermal behaviour of the observed alloy phases during the annealing process obtained from *in situ* Mössbauer measurements, performed in a high vacuum furnace. The results indicate that the a-Fe_2B phase has its relative volume fraction reduced from 73% to about 50%, while the fraction of the bcc-Fe phase has increased from 10 to 23%, for annealing temperature values up to 573 K. For annealing temperatures above 675 K, the fraction of the bcc-Fe phase decreases to 12%, while the relative area associated with the a-Fe_2B phase increases back to about 60%. The high temperature increase of the amorphous phase content is intriguing and may be due to: (a) the Fe atoms from the n-Fe phase having diffused into the a-Fe_2B phase, increasing its Fe content, or (b) the n-Fe phase having reacted with free boron atoms in the annealing process, forming a rich Fe/B phase. These arguments
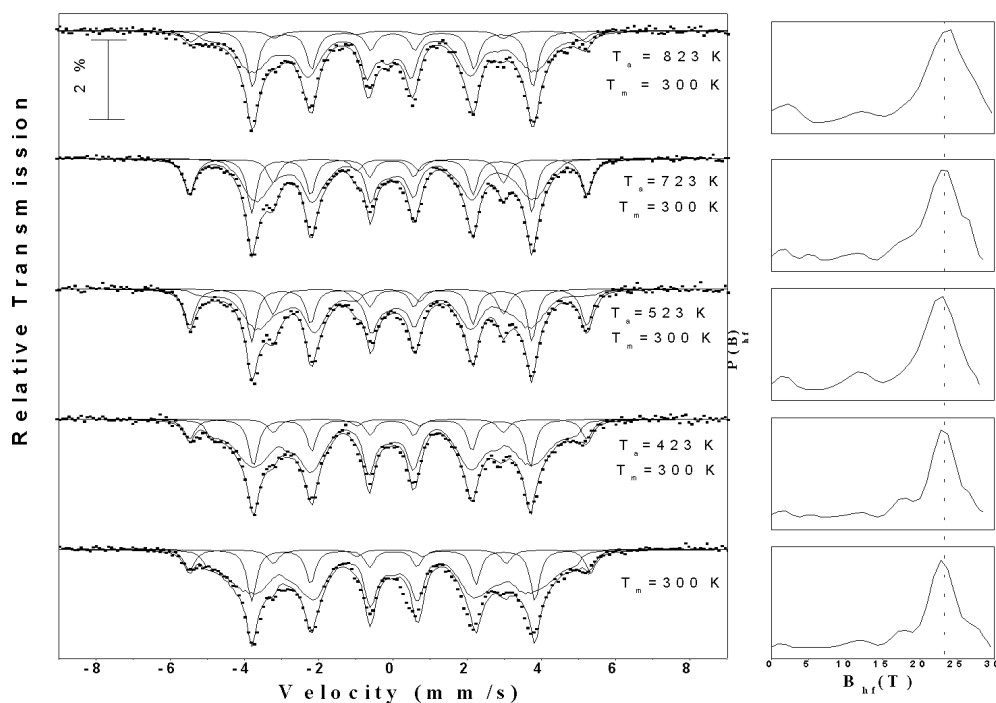
Figure 3. Mössbauer spectra at 300 K (T_m) of the as-milled Fe$_{67}$B$_{33}$ alloy (sample A) and annealed at indicated temperatures (T_a) in a high vacuum Mössbauer furnace (sample B).

may be related to the observed slightly broader magnetic hyperfine field distribution curve of sample B annealed at 823 K compared with, for example, that annealed at 723 K (figure 3, right-hand side). On the other hand, the initial n-Fe$_2$B phase shows a systematic increase of its relative volume fraction for annealing temperatures lower than 623 K, but it remains unchanged for higher temperatures. This temperature behaviour observed for the S2 subspectrum may be mainly associated with the appearance of the Fe$_3$B phase, observed in the XRD pattern of sample B, after it has been annealed at 823 K (see figure 5(a)). However, as reported by Shánchez *et al* (1989) the Fe$_2$B and Fe$_3$B phases cannot be distinguished by Mössbauer experiments at 300 K due to the similarity of their hyperfine parameter values. In this case, the Mössbauer fittings were done with one broad sextet, convoluting these two component subspectra.

Figure 6 shows the Mössbauer spectra of sample C obtained at 300 K for three different annealing temperatures. The Mössbauer spectra of sample C, annealed at temperatures lower than 923 K, are analysed with the same three subspectra used to fit the Mössbauer spectra of samples A and B, but with different Mössbauer relative volume fractions. In this case, the content of α-Fe phase systematically increases with annealing temperature. The Mössbauer spectrum of sample C annealed at 923 K is fitted with only crystalline components associated with the Fe, Fe$_2$B and Fe$_3$B phases, in agreement with the XRD result shown in figure 5(b). On the other hand, comparing the relative volume fraction of the α-Fe phase observed in samples B and C, at similar annealing temperatures (423 or 623 K), the alloy annealed in a quartz tube presents segregation (Fe) and crystallization (Fe$_2$B and/or Fe$_3$B) effects higher than in the case of the alloy annealed in the vacuum furnace. This observation may indicate that these effects had been enhanced by the presence of oxygen in the residual atmosphere,
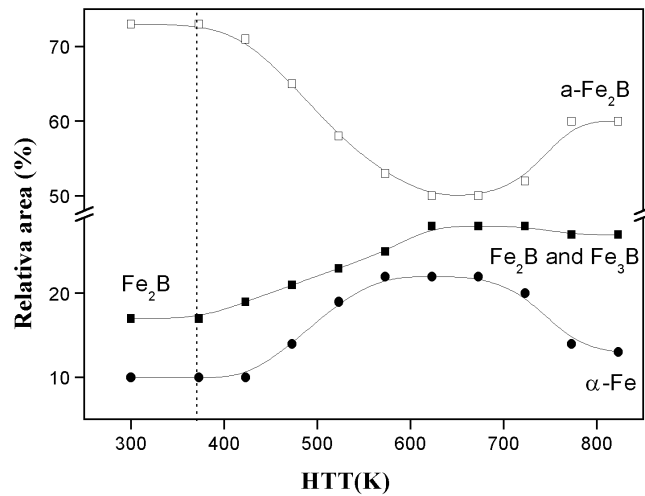
Figure 4. Temperature dependence behaviour of the Mössbauer relative absorption area associated with different phases observed in as-milled $Fe_{67}B_{33}$ alloy (sample A) submitted to an annealing process in a high vacuum Mössbauer furnace. The vertical dotted line separates the region of n-Fe_2B from that one, where the two phases (Fe_2B and Fe_3B) coexist. The lines connecting the points are guides for the eyes.
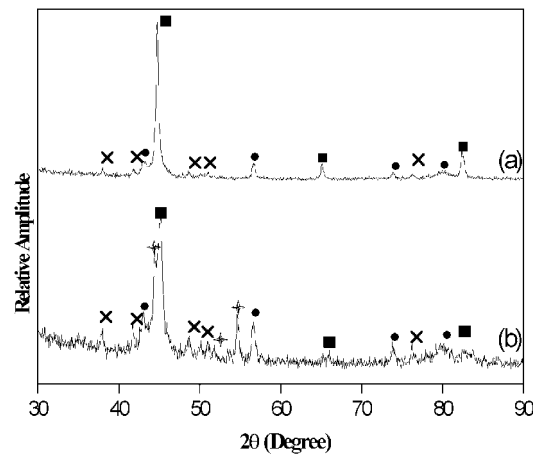

Figure 5. XRD patterns of sample B annealed at 823 K (a) and sample C annealed at 923 K (b). The symbols ■, ●, × and + correspond to α-Fe, Fe_2B, Fe_3B and graphite, respectively. Graphite powders (+) were added to fill the Mössbauer sample holder.

during the annealing process, probably leading to an oxidation of boron atoms. This hypothesis may be supported by the report of Linderoth (1992) that observed the oxidation of boron, the segregation (Fe) and the crystallization (Fe_2B and/or Fe_3B) effects in an ultrafine a-Fe/B alloy prepared by chemical methods and annealed over a similar temperature range. Thus, the present results may suggest that the better residual pressure expected for sample B leads to a lower Fe segregation and Fe_2B crystallization processes than in the case of sample C.

However, concerning the annealing process of samples B and C, it deserves further comment: the XRD pattern shows evidence of the Fe_3B phase present in the samples annealed
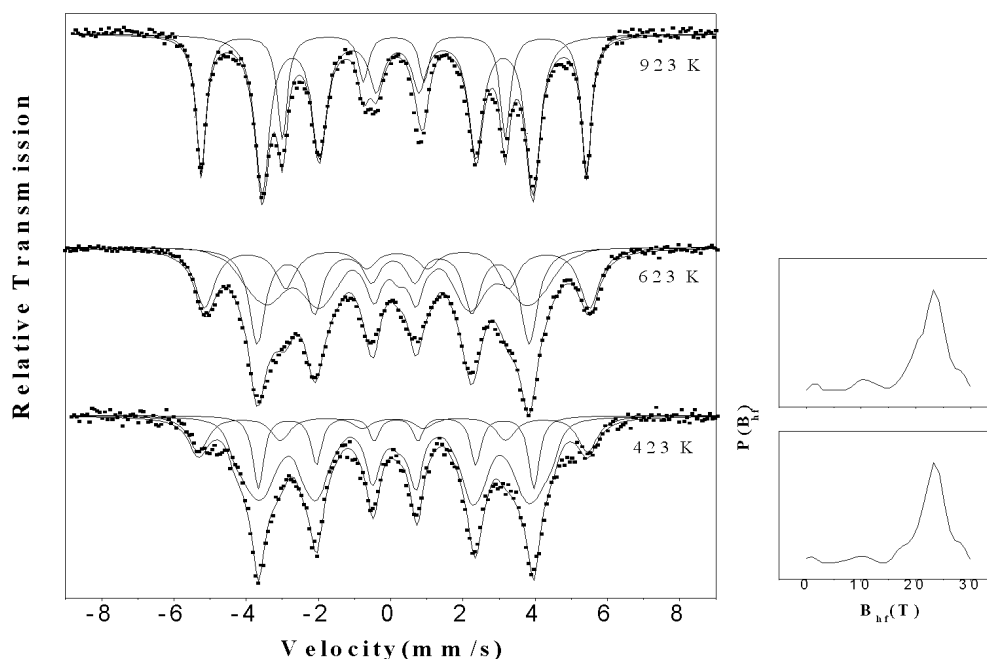
Figure 6. 300 K Mössbauer spectra of the as-milled $Fe_{67}B_{33}$ alloy sealed under vacuum in a quartz tube and annealed at different temperatures in a tubular resistive furnace (sample C).

at temperatures about 623 K (sample C). On the other hand, the formation of the Fe_3B phase occurred in the temperature range from 373–623 K in sample B since, at these temperatures, the relative volume fraction of the S2 subspectrum is enhanced for increasing temperature. Therefore, the low temperature DSC peaks (figure 2) may be due to a boron oxidation process that yields rich Fe phases, i.e. α-Fe and Fe_3B phases, as indicated by the present Mössbauer results for temperatures lower than 623 K (see figure 4) and already commented on, instead of the early surface crystallization effect suggested by Jing *et al* (1991).

In order to investigate some magnetic properties of sample B, after it had been annealed at 823 K, high temperature Mössbauer measurements were performed. The temperature range was selected according with two main points: (1) to provide distinct Fe_2B and F_3B phases, fitted with the S2 subspectrum and (2) to avoid an amorphous–crystalline transition.

The Mössbauer spectra of sample B, annealed at 823 K and measured at different temperatures, are shown in figure 7. The spectrum measured at 723 K is fitted with two magnetic and one paramagnetic subspectra: the n-Fe (S1) and the a-Fe₂B (distribution component) plus one doublet (D1). At this temperature, the D1 subspectrum has almost the same relative volume fraction as the S2 one, associated with the Fe_2B and Fe_3B phases, indicating that these phases are in the paramagnetic state. Again, the relative fractions of the Fe_2B and Fe_3B phases could not be distinguished. However, it is important to mention that the Curie temperature (T_C) of the Fe_3B ordered phase is about 820 K (Chien *et al* 1979), while that of the Fe_2B compound is 1015 K (Candeville and Meyer 1962). The unexpected paramagnetic states of these phases will be discussed below. On the other hand, increasing the temperature from 723 to 773 K, one can observe that the n-Fe has its B_{hf} values 'almost' constant (as shown by the vertical broken lines in figure 7), but with its relative fraction smaller than the value obtained at 723 K. At 823 K, the Mössbauer spectrum of the sample B alloy shows practically
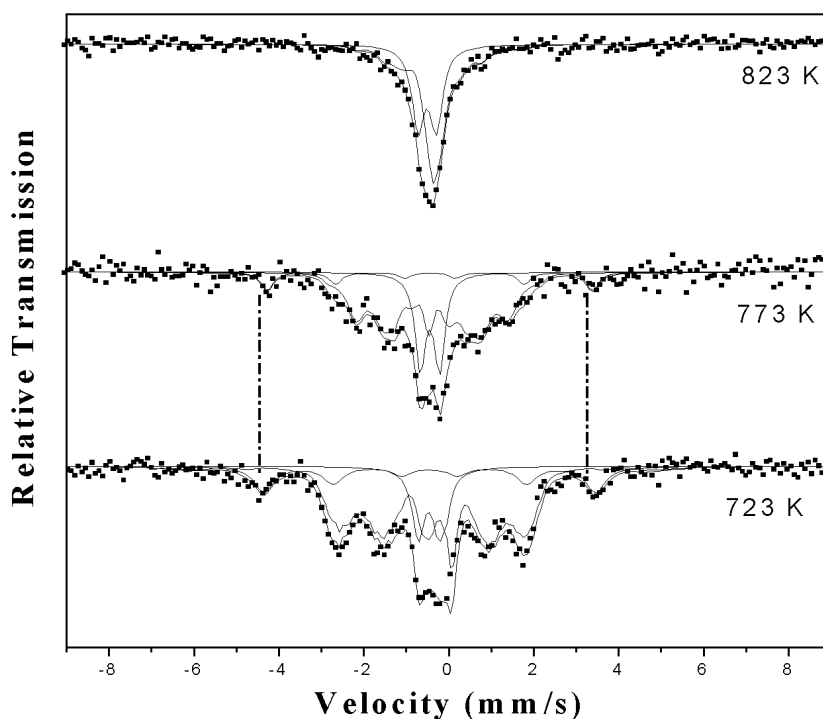
Figure 7. Mössbauer spectra of the $Fe_{0.67}B_{0.33}$ alloy (sample B) at indicated temperatures after it has been annealed at 823 K. The Mössbauer spectra are plotted relative to the Mössbauer source kept at RT.

a paramagnetic state. Thus, the abrupt reduction of the B_{hf} values indicates that the α-Fe, Fe_2B and Fe_3B phases behave like small superparamagnetic particles over this temperature range (723–823 K). Furthermore, the n-Fe particles may have a broad distribution of particle sizes, with blocking temperature in the range 773–823 K, while the Fe_2B and Fe_3B phases may have their blocking temperature values lower or equal to 723 K. Finally, the T_C value of the a-Fe_2B phase is about 823 K, as indicated by Mössbauer data. This T_C value fits into the systematic of those values observed for a-Fe/B ribbons, at higher boron concentration region reported by Chien *et al* (1979).

Thus, with the results presented above one may say that the milled $Fe_{67}B_{33}$ alloy submitted to an annealing process at 823 K is a multiphase nanostructured material having small magnetic particles of α-Fe, Fe_2B and Fe_3B dispersed in the a-Fe_2B matrix.

4. Conclusion

In the present paper a large amount of an amorphous a-Fe_2B phase has been produced by HEM using specific milling tools, in contrast with the results reported by Jing *et al* (1991) and Yang *et al* (1999). The final milled alloy is composed of 73% a-Fe_2B, 10% n-Fe and 17% n-Fe_2B. The higher segregated Fe fraction, reported in the literature for an Fe_2B alloy obtained by a milling technique (Balogh *et al* 1997) or yielded during its annealing process (Linderoth 1992), may be enhanced due to boron oxidation caused by a contaminated residual atmosphere. A higher Fe segregation effect is observed in the case of samples heat treated in a

sealed quartz tube (sample C) when compared with the case where the sample atmosphere had been continuously pumped during the heat treatment (sample B). High temperature Mössbauer measurements indicate that the α-Fe, Fe$_2$B and Fe$_3$B phases thermally precipitated behave like small superparamagnetic particles in the temperature range 723–823 K. For the present results, the estimated T$_C$ value for the a-Fe$_2$B phase is 823 K and it fits into the systematic reported for a-Fe/B ribbons with higher B concentration.

Acknowledgments

References

Balogh J, Bujdoso L, Kemeny T and Vincze I 1997 *J. Phys.: Condens. Matter* **9** L503
Cadeville M C and Meyer A J P 1962 *C. R. Acad. Sci., Paris* **255** 339
Chien C L, Musser D, Gyorgy E M, Sherwood R C, Chen H S, Luborsky F E and Walter J L 1979 *Phys. Rev.* B **20** 283
Chong-Oh K, Taik-Kee K and Miroku T 1981 *Proc. 4th Int. Conf. on Rapid Quenched Metals (Sendai, 1981)* ed
    T Masumoto and K Suzuki (Sendai: The Japan Institute of Metals) p 173
Jing J, Calka A and Campbell S J 1991 *J. Phys.: Condens. Matter* **3** 7413
Larica C, Alves K M B, Baggio-Saitovitch E and Guimarães A P 1995 *J. Magn. Magn. Mater.* **145** 306
Linderoth S 1992 *J. Magn. Magn. Mater.* **104–7** 128
Murphy K A and Hershkowitz N 1973 *Phys. Rev.* B **7** 23
Shánchez F H and Fernández Van Raap M B 1992 *Phys. Rev.* B **46** 13 881
Shánchez F H, Zhang Y D, Budwick J I and Haseguawa R 1989 *J. Appl. Phys.* **66** 1671
Yang Y Z, Li Q S, Zhu Y L, Ma X M and Dong Y D 1999 *J. Mater. Technol.* **15** 137
Waba H and Shiba M 1993 *Nucl. Instrum. Methods* **76** 301
Xia S K, Baggio-Saitovitch, Rodriguez V A, Passamani E C, Takeuchi A Y, Ghafari M, Avillez and Rizzo Assunção
    1996 *J. Alloys Compounds* **242** 85